Table 2
Brain areas manifesting significant decrease of FA and gray matter volumes in the patient.

Region	MNI (*x*,*y*,*z*)	Voxels	*Z* score
FA			
Left superior longitudinal fasciculus	−20, −36, 48	335	6.23
Left thalamic radiation	−18, −10, 14	189	5.42
Right thalamic radiation	16, −18, 4	816	5.88
Gray matter volume			
Middle cingulate cortex	10, −20, 46	158	5.50
Right inferior parietal cortex	56, −38, 50	96	4.77
Medial occipital cortex	2, −90, −8	133	4.74
Hypothalamus	0, 10, −6	97	4.66
Left insular cortex	−50, −4, 4	67	4.58
	−36, −22, 12	182	4.45
Right insular cortex	42, −10, 12	64	4.49

significantly smaller FA values in the left superior longitudinal fasciculus and bilateral thalamic radiation including the fasciculus between the brain stem and the cortical regions via the thalamus.

From the voxel-based morphometry results, we found regional decrease of gray matter volumes in the patient. The patient showed significantly smaller gray matter volumes in the bilateral insular cortex, posterior cingulate cortex, hypothalamus, right parietal cortex and medial occipital cortex (Fig. 3, Table 2).

As shown in Fig. 4, in the patient, a significant decrease in regional cerebral blood flow, in broad cortical areas including the ventromedial prefrontal cortex (VM), was revealed by Tc-ECD SPECT.

4. Discussion

The patient showed behavioral problems following cerebral injury from a traffic accident. The patient performed normally on a variety of neuropsychological tests, but had an abnormal outcome on IGT, which assesses the decision-making process. The patient's problem may stem from insensitivity to future consequences, positive or negative, as a result being primarily guided by immediate prospects. This 'myopia for the future' of the patient may persist in the face of a problematic behavior pattern that should result in severe adverse consequences.

DTI-MRI results showed that the patient had a significant decrease of FA in the fasciculus between the brain stem and insula via the thalamus. To the extent that FA is related to axonal integrity, density, caliber and myelination, our findings of a subnormal level of FA suggest the presence of microstructural abnormalities in the fasciculus of the patient. Damasio et al. proposed that somatic feedback helps guide the decision-making process in humans—the somatic-marker hypothesis (SMH) (Damasio, 1994). Evidence in favor of this hypothesis was provided by a study demonstrating that cerebrally intact individuals with peripheral neuropathy showed abnormal decision-making in IGT, suggesting that the peripheral neuropathy resulted in reduced afferent feedback to the brain (Bechara et al., 1998). In terms of SMH, microstructural abnormalities in the fasciculus of the patient resulted in reduced afferent feedback to the brain, resulting in less efficient decision-making.

When we focused on the cortical gray matter changes, we found significant decrease in gray matter volumes in the bilateral insular cortex, hypothalamus, posterior cingulate cortex, medial occipital and right parietal cortex, possibly reflecting Wallerian degeneration secondary to the microstructural abnormalities in the fasciculus. These atrophic regions may be a part of neural networks connected with the brain stem by the damaged fasciculus, which is related to the decision-making process.

Recently, Damasio et al. proposed the hypothesis that feelings first emerge from the integrated operation of structures in the brain stem and hypothalamus. The activity patterns present in

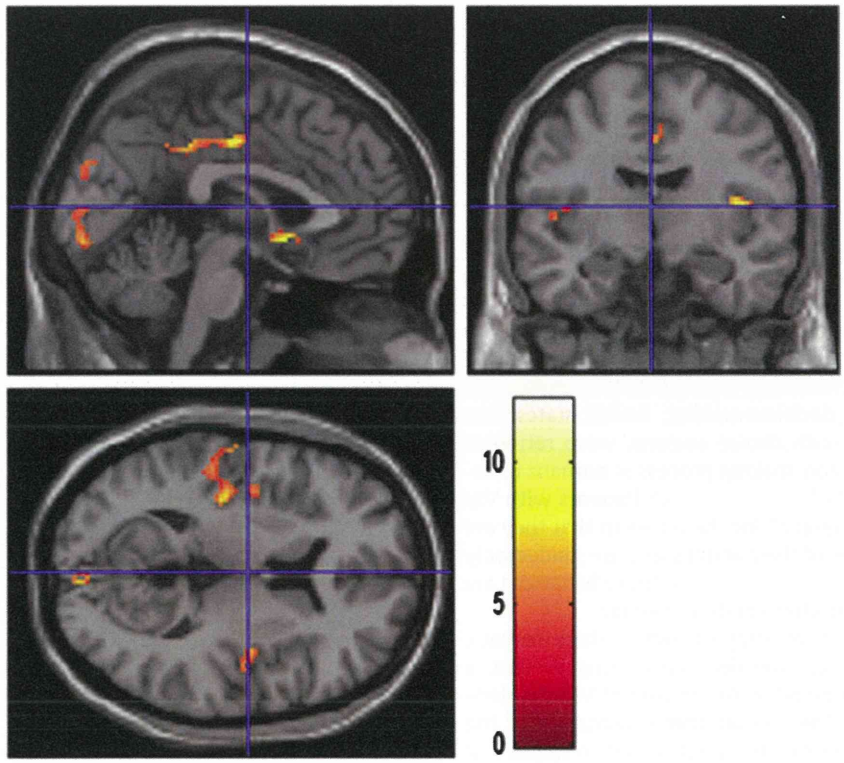

Fig. 3. Significant decrease of gray matter volumes in the patient compared to healthy controls. Detected areas exceed uncorrected p value of 0.001 with 50 or more contiguous voxels. These statistical parametric mapping projections were then superimposed on representative transaxial ($z = 10$), sagittal ($x = 0$), and coronal ($y = -11$) magnetic resonance images.

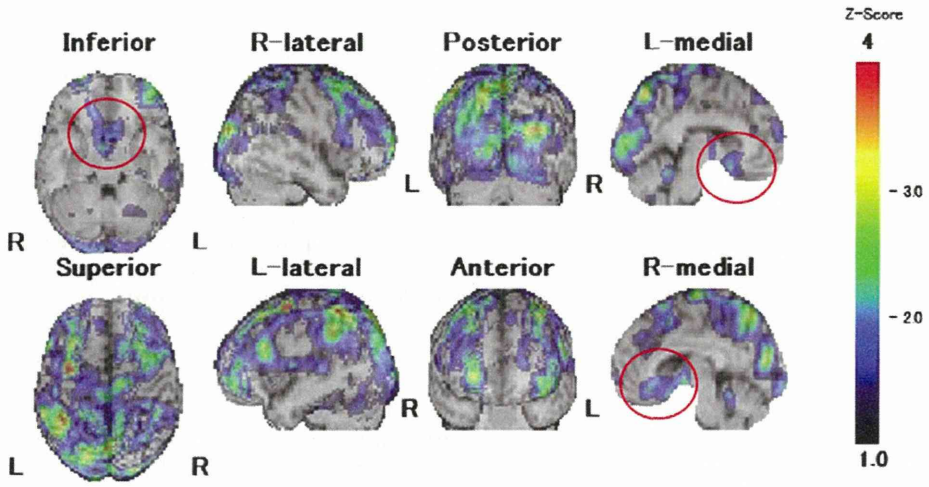

Fig. 4. Tc-99m ECD-SPECT results statistically analyzed by comparing with standard SPECT images obtained from easy *Z*-score imaging system; eZIS. Hypoperfusioned areas showing more than 2SD deviation from the standard SPECT images were 3D-rendered on brain template. The area shown in the red circle is the ventromedial prefrontal cortex (VM).

the insular cortex during feeling states would constitute a second-order mapping of activity patterns first assembled subcortically. The information contained in insular maps would be suitable for interaction with information in cortical systems involved in sensory processing (including visuo-perceptual processing in parieto-occipital cortex) and in higher-order functions such as decision-making (Damasio, Damasio, & Tranel, 2012). The posterior cingulate cortex is related to emotional processing via its connection with the insular cortex (Immordino-Yang, McColl, Damasio, & Damasio, 2009; Parvizi, Van Hoesen, Buckwalter, & Damasio, 2006). The atrophic change of cortical and subcortical regions and their disconnection with the brain stem may disturb the efficient generation of feelings accompanying anticipation, which is necessary for the final decision.

By SPECT, there was a significant blood flow decrease in the broad cortical areas. There is a possibility that the presence of microstructural abnormalities in the fasciculus, which projects to these areas, caused the inactivity of cortical function. In these areas, a significant decrease of blood flow in VM should be regarded as important, although there was no significant cortical change according to MRI. VM has been widely recognized as playing a critical role in successful decision-making, fueled in part by well-studied single cases (Cato, Delis, Abildskov, & Bigler, 2004; Dimitrov, Phipps, Zahn, & Grafman, 1999; Eslinger & Damasio, 1985).

The insular cortex has extensive reciprocal connectivity with VM (Augustine, 1996; Ongür & Price, 2000), and inactivity of the insular cortex may also decrease the activity of the VM region. SMH proposed that during decision-making, bodily states that were previously associated with choice options, were retrieved by VM, and it guides the decision-making process in humans in situations of risk and complexity (Damasio, 1994). Patients with VM lesions are known to have "myopia" for the future in that they are oblivious to the consequences of their actions and are guided only by immediate prospects (Bechara et al., 1994). These behaviors are similar to those of our patient after cerebral damage.

While our findings seemed to support SMH, where somatic feedback to the brain influences the decision-making process, a note of caution must be expressed as to the role of VM for decision-making process in IGT. There is another explanation of the failure of patients with VM lesions to perform well in the IGT. It was suggested that the difficulties of the patient with VM lesions might be due to a deficit in reversal learning – the ability to adjust their responses when the reinforcement values of stimuli are reversed (Maia & McClelland, 2005). It was argued that the difficulties of patients with VM lesions in IGT performance can be explained by an inability to reverse a learned contingency (Clark, Cools, & Robbins, 2004; Fellows & Farah, 2005; Maia & McClelland, 2004, 2005). We require additional empirical support to clarify the role of VM in the SMH.

In conclusion, we can postulate that the patient had a dysfunction of the decision-making process. Inefficiency of the decision-making process is likely to be related to the patient's problematic behavior after the traffic accident. The microstructural abnormality in the fasciculus, which may have resulted from the traffic accident, caused reduced afferent feedback to the brain, resulting in less efficient decision-making. Our findings seem to support SMH, where somatic feedback to the brain influences the decision-making process. Dysfunction of cortical and subcortical regions disconnected from the brain stem may also disturb the efficient generation of the feelings from somatic feedback, which is necessary for the final decision.

References

Augustine, J. R. (1996). Circuitry and functional aspects of the insular lobe in primates including humans. *Brain Research. Brain Research Reviews, 22*, 229–244.

Bechara, A., Damasio, A. R., Damasio, H., & Anderson, S. W. (1994). Insensitivity to future consequences following damage to human prefrontal cortex. *Cognition, 50*, 7–15.

Bechara, A., Tranel, D., Wilson, J., Heberlein, A. S., Ross, M., & Damasio, A. R. (1998). Impaired decision-making in peripheral neuroopathy. *Society for Neuroscience Abstracts, 24*, 1176.

Berg, E. A. (1948). A simple objective test for measuring flexibility in thinking. *The Journal of General Psychology, 39*, 15–22.

Borkowski, J. G., Benton, A. L., & Spreen, O. (1967). Word fluency and brain damage. *Neuropsychologia, 5*, 135–140.

Cato, M. A., Delis, D. C., Abildskov, T. J., & Bigler, E. (2004). Assessing the elusive cognitive deficits associated with ventromedial prefrontal damage: A case of a modern-day Phineas Gage. *Journal of the International Neuropsychological Society, 10*, 453–465.

Clark, L., Cools, R., & Robbins, T. W. (2004). The neuropsychology of ventral prefrontal cortex: Decision-making and reversal learning. *Brain and Cognition, 55*, 41–53.

Crosson, B., Novack, T. A., Trenerry, M. R., & Craig, P. L. (1988). California Verbal Learning Test (CVLT) performance in severely head-injured and neurologically normal adult males. *Journal of Clinical and Experimental Neuropsychology, 10*, 754–768.

Damasio, A. R. (1994). *Descartes' Error*. London: Papermac/Macmillan.

Damasio, A. R., Damasio, H., & Tranel, D. (2012). Persistence of feelings and sentience after bilateral damage of the insula. *Cerebral Cortex, 23*, 833–846.

Dimitrov, M., Phipps, M., Zahn, T. P., & Grafman, J. (1999). *A thoroughly modern Gage Neurocase, 5*, 345–354.

Dombovy, M. L., & Olek, A. C. (1997). Recovery and rehabilitation following traumatic brain injury. *Brain Injury, 11*, 305–318.
Dubois, B., Slachevsky, A., Litvan, I., & Pillon, B. (2000). The FAB: A frontal assessment battery at bedside. *Neurology, 55*, 1621–1626.
Eslinger, P. J., & Damasio, A. R. (1985). Severe disturbance of higher cognition after bilateral frontal lobe ablation: Patient EVR. *Neurology, 35*, 1731–1741.
Fellows, L. K., & Farah, M. J. (2005). Different underlying impairments in decision-making following ventromedial and dorsolateral frontal lobe damage in humans. *Cerebral Cortex, 15*, 58–63.
Immordino-Yang, M. H., McColl, A., Damasio, H., & Damasio, A. (2009). Neural correlates of admiration and compassion. *Proceedings of the National Academy of Sciences of the United States of America, 106*, 8021–8026.
Levine, B., Black, S. E., Cheung, G., Campbell, A., O'Toole, C., & Schwartz, M. L. (2005). Gambling task performance in traumatic brain injury: Relationships to injury severity, atrophy, lesion location, and cognitive and psychosocial outcome. *Cognitive and Behavioral Neurology, 18*, 45–54.
Maia, T. V., & McClelland, J. L. (2004). A reexamination of the evidence for the somatic marker hypothesis: What participants really know in the Iowa gambling task. *Proceedings of the National Academy of Sciences of the United States of America, 101*, 16075–16080.
Maia, T. V., & McClelland, J. L. (2005). The somatic marker hypothesis: Still many questions but no answers. *Trends in Cognitive Science, 9*, 162–164.
Masutani, Y., Aoki, S., Abe, O., Hayashi, N., & Otomo, K. (2003). MR diffusion tensor imaging: Recent advance and new techniques for diffusion tensor visualization. *European Journal of Radiology, 46*, 53–66.
Mizumura, S., & Kumita, S. (2006). Stereotactic statistical imaging analysis of the brain using the easy Z-score imaging system for sharing a normal database. *Radiation Medicine, 24*, 545–552.
Ongür, D., & Price, J. L. (2000). The organization of networks within the orbital and medial prefrontal cortex of rats, monkeys and humans. *Cerebral Cortex, 10*, 206–219.
Parvizi, J., Van Hoesen, G. W., Buckwalter, J., & Damasio, A. (2006). Neural connections of the posteromedial cortex in the macaque. *Proceedings of the National Academy of Sciences of the United States of America, 103*, 1563–1568.
Raven, J. C. (1958). *Guide to the standard progressive matrices*. London: HK Lewis.
Santoro, J., & Spiers, M. (1994). Social cognitive factors in brain injury-associated personality change. *Brain Injury, 8*, 265–276.
Spreen, O., & Strauss, E. (1991). *A conpendium of neuropsychological tests*. Oxford: Oxford University Press.
Stroop, J. (1935). Studies of interference in serial verbal reactions. *Journal of Experimental Psychology, 18*, 643–662.
Stuss, D. T., & Gow, C. A. (1992). "Frontal dysfunction" after traumatic brain injury. *Neuropsychiatry, Neuropsychology and Behavior Neurology, 5*, 272–282.
Stuss, D. T., Stethem, L. L., Hugenholtz, H., Picton, T., Pivik, J., & Richard, M. T. (1989). Reaction time after head injury: Fatigue, divided and focused attention, and consistency of performance. *Journal of Neurology, Neurosurgery and Psychiatry, 52*, 742–748.
Warriner, E. M., & Velikonja, D. (2006). Psychiatric disturbances after traumatic brain injury: Neurobehavioral and personality changes. *Current Psychiatry Reports, 8*, 73–80.
Wechsler, D. (1981). *WAIS-R manual*. New York: Psychological Corporation.
Wechsler, D. (1987). *Wechsler memory scale-revised*. San Antonio: Harcourt Brace Jovanovich.
Wilson, B. A., Alderman, N., Burgess, P. W., Emslie, H. C., & Evans, J. J. (1996). *The behavioural assessment of the dysexecutive syndrome*. Flempton: Thames Valley Test Company.
Yody, B. B., Schaub, C., Conway, J., Peters, S., Strauss, D., & Helsinger, S. (2000). Applied behavior management and acquired brain injury: Approaches and assessment. *The Journal of Head Trauma Rehabilitation, 15*, 1041–1060.

Available online at www.sciencedirect.com
SciVerse ScienceDirect
www.elsevier.com/locate/brainres

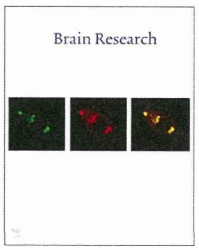

Research Report

Longitudinal white matter changes in Alzheimer's disease: A tractography-based analysis study

Soichiro Kitamura[a,*], Kuniaki Kiuchi[a], Toshiaki Taoka[b], Kazumichi Hashimoto[a], Shotaro Ueda[a], Fumihiko Yasuno[a], Masayuki Morikawa[a,c], Kimihiko Kichikawa[b], Toshifumi Kishimoto[a]

[a]Department of Psychiatry, Nara Medical University, Kashihara, Japan
[b]Department of Radiology, Nara Medical University, Kashihara, Japan
[c]Sakai City Mental Health Center, Sakai, Japan

ARTICLE INFO

Article history:
Accepted 29 March 2013
Available online 10 April 2013

Keywords:
Alzheimer's disease
Dementia
Diffusion tensor imaging
Disease progression
Tract-based analysis

ABSTRACT

Alzheimer's disease (AD) classically presents with gray matter atrophy, as well as feature significant white matter abnormalities. Previous evidence indicates the overall burden of these pathological changes continues to advance as the disease progresses. The aim of this study was to investigate whether pathological alterations of white matter tracts correlate with the course of AD disease progression. 35 AD patients and 29 normal controls were recruited to the study and administered baseline magnetic resonance diffusion tensor imaging (DTI) acquisition and a cognitive function assessment at the time of initial evaluation. Subjects were re-evaluated with secondary DTI scan and cognitive function assessment at intervals of about 1.5 years on average. For the DTI acquired scans, we calculated diffusion tensor parameters, fractional anisotropy (FA), apparent diffusion coefficient (ADC), radial diffusivity (DR), and axial diffusivity (DA) along with the uncinate fasciculus (UNC), the inferior longitudinal fasciculus (ILF), and the inferior occipitofrontal fasciculus (IOFF). Compared to baseline, a significant mean FA reduction of the bilateral UNC, as well as a significant mean DR increase of the left UNC, was evident in AD patients at follow-up. Compared with normal controls, AD patients exhibited significant diffusion parameter abnormalities in their UNC, ILF, and IOFF. Taken together, these results indicate

Abbreviations: AD, Alzheimer's disease; MTL, medial temporal lobe; DTI, Diffusion tensor imaging; ROI, region of interest; VBA, voxel-based morphometric analysis; MRI, magnetic resonance imaging; UNC, uncinate fasciculus; ILF, inferior longitudinal fasciculus; IOFF, inferior occipitofrontal fasciculus; FA, fractional anisotropy; ADC, apparent diffusion coefficient; D_A, axial diffusivity; D_R, radial diffusivity; MMSE, Mini Mental State Examination; ADAS-Cog, Alzheimer's Disease Assessment Scale-cognitive component-Japanese version; NINCDS-ADRDA, National Institute of Neurological and Communicative Disorders and Stroke and the Alzheimer's Disease and Related Disorders Association; TR, repetition time; TE, echo time; ANOVA, analysis of variance

*Correspondence to: Department of Psychiatry, Nara Medical University, 840 Shijo-cho, Kashihara, Nara 634-8522, Japan. Fax: +81 744 22 3854.
E-mail addresses: kitaso@naramed-u.ac.jp (S. Kitamura), kuniaki@naramed-u.ac.jp (K. Kiuchi), ttaoka@naramed-u.ac.jp (T. Taoka), hkaz@naramed-u.ac.jp (K. Hashimoto), shotaro@naramed-u.ac.jp (S. Ueda), yasunof@naramed-u.ac.jp (F. Yasuno), AV6M-MRKW@j.asahi-net.or.jp (M. Morikawa), kkichika@naramed-u.ac.jp (K. Kichikawa), toshik@naramed-u.ac.jp (T. Kishimoto).

0006-8993/$ - see front matter
http://dx.doi.org/10.1016/j.brainres.2013.03.052

that progressive pathological white matter alterations can be quantified using the DTI parameters utilized here and may prove to be a useful biological marker for monitoring the pathophysiological course of AD.

1. Introduction

Alzheimer's disease (AD) is the most common cause of dementia, and the number of AD patients have been increasing in recent years. AD shows symptoms of memory impairment and disturbance in orientation in its early stage, and then shows further higher brain dysfunction, such as visuospatial disturbance and executive dysfunction with disease progression. AD shows brain atrophy with disease progression. In imaging studies of AD, it has been shown that the medial temporal lobe (MTL) structures become atrophied in the early stage, and further atrophy progressively spreads to the neocortical regions. Although AD is considered to affect mainly the cortical gray matter, pathological changes are also observed in the white matter, such as the loss of axons and oligodendrocytes together with reactive astrocytosis (Kobayashi et al., 2002; Roth et al., 2005). The executive function is consequent on activating the interaction across the several cortical regions, and it is considered that white matter abnormalities are related to the various cognitive dysfunction (Delbeuck et al., 2007; Fellgiebel et al., 2008; Bozzali et al., 2011). Therefore, the neural connectivities across brain regions are important to comprehend the pathophysiology of AD.

Diffusion tensor imaging (DTI) is based on evaluating the random motion of water molecules, and can noninvasively examine neural microstructural tissue organization. In region of interest (ROI) analysis, microstructural damage is shown in the frontal, temporal regions or in the hippocampus in AD (Chen et al., 2009; Hong et al., 2010). The voxel-based morphometric analysis (VBA) in AD is known to show abnormality in the medial temporal structure and the hippocampus (Di. Paola et al., 2007; Rose et al., 2008). Furthermore, the tract-based analysis, which extracts the diffusion parameters along the reconstructed white matter bundles, shows microstructural damage in the uncinate fasciculus, cingulated fasciculus, and the corpus callosum (Kiuchi et al., 2009; Nakata et al., 2008; Pievani et al., 2010; Yasmin et al., 2008). Also, AD is a progressive neurodegenerative disease and shows atrophic changes and various clinical symptoms with disease progression. Matsuda et al. (2002) reported that progressive medial temporal lobe atrophy in a 3 dimension-magnetic resonance imaging (MRI) follow-up study was investigated in AD patients. Taken together, the research on longitudinal white matter changes would be important to understand AD pathophysiology. However, to the best of our knowledge, a follow-up DTI study for white matter changes in AD has not been conducted.

In this study, we followed AD patients from the early stage to the moderate, and investigated their longitudinal white matter changes with disease progression. In the course of AD, pathological neuronal change begins in the medial temporal regions such as enthorhinal cortex, hippocampus and parahippocampus, which subsequently spreads to the neocortical regions with temporal, parietal and frontal cortex (Braak and Braak, 1995). Thus, pathological alterations in AD occur in temporal regions of the brain. Therefore, in recent study, we investigated three major white matter bundles, the uncinate fasciculus (UNC), the inferior longitudinal fasciculus (ILF) and the inferior occipitofrontal fasciculus (IOFF). The UNC is considered to play an important role in memory and cognition (Highley et al., 2002), and the ILF and IOFF are related to executive functions such as emotional process, object cognition, verbal and visual memory and visuospatial cognition (Chanraud et al., 2010; Kiuchi et al., 2010; Kringelbach, 2005). We hypothesized that the disruption in major white matter bundles can cause memory impairment or high cognitive impairments, and the connectivity of white matter tracts is impaired with disease progression.

In this study, we employed tract-based analysis to examine microstructural white matter changes with several major tracts in AD patients. Tract based analysis assembles the local diffusion tensor data into tracts using scalar metrics, such as fractional anisotropy (FA) and apparent diffusion coefficient (ADC). Furthermore, the coordinates of the tensor matrix can be diagonalized to extract the three eigenvalues; λ_1, λ_2, and λ_3 derived from the main eigenvectors of diffusion elements. The combination of these eigenvalues defines diffusion parameters, the axial diffusivity (D_A), in parallel with axon fibers, and radial diffusivity (D_R), perpendicular to axon fibers (Basser and Pierpaoli, 1998; Song et al., 2002; Sun et al., 2005). Thus, tract-based analysis can evaluate the specific anatomical localization of a single tract and allow measurement throughout the length of the bundles.

2. Results

2.1. *demographic data*

The demographic and neuropsychological characteristics are shown in Table 1. No significant differences were noted in age and educational level between AD patients and normal controls. Between baseline and follow-up, AD patients showed significant decline in Mini Mental state Examination (MMSE) and Alzheimer's Disease Assessment Scale-cognitive component-Japanese version (ADAS-Cog.) scores ($p<0.005$).

2.2. *FA and ADC*

Table 2 shows the FA and ADC values of the UNC, ILF and IOFF for all the groups. Among the AD patients, compared with baseline point, the significant mean FA reduction of the bilateral UNC was shown at follow-up point (right, $p<0.05$; left, $p<0.01$). In contrast, no other metrics were significant between baseline and follow-up point. Compared with the normal controls, we found the significant mean FA reduction of the bilateral UNC (right, $p<0.001$; left, $p<0.001$), and the

Table 1 – Demograpahic and clinical data of the Alzherimer's disease patients and normal controls.

	AD		NC	p
	Baseline	Follow		
Number (Male/Female)	35 (11/24)	35 (11/24)	29 (12/17)	
Age, mean (SD), y	75.3 (4.74)		73.3 (9.37)	N.S.
Education, mean (SD), y	11.7 (2.05)		11.5 (2.36)	N.S.
MMSE, mean (SD)	22.1 (2.28)	19.1 (3.20)	27.9 (2.13)	<0.001
ADAS, mean (SD)	15.7 (5.77)	20.8 (7.42)		0.002

MMSE, Mini Mental State Examination; ADAS, Alzheimer's disease assessment scale- cognitive subscale; NC, normal controls; AD, Alzheimer's disease; N.S., not significant.

Table 2 – The mean FA and ADC of the UNC, ILF and IOFF, and statistical analysis among all the groups.

Variable	Group			One-way ANOVA		Post-hoc Bonferroni test, p value		
	AD Baseline	AD Follow	NC	F	p value	AD Baseline vs. AD Follow	AD Baseline vs. NC	AD Follow vs. NC
UNC								
FA, R, mean (SD)	0.371 (0.101)	0.359 (0.023)	0.394 (0.018)	32.2	<0.001	0.013*	<0.001***	<0.001***
L, mean (SD)	0.367 (0.015)	0.351 (0.026)	0.397 (0.021)	37.6	<0.001	0.005**	<0.001***	<0.001***
ADC, R, mean (SD)	0.429 (0.017)	0.437 (0.025)	0.410 (0.016)	14.5	<0.001	N.S.	0.001**	<0.001***
L, mean (SD)	0.431 (0.021)	0.439 (0.024)	0.411 (0.014)	15.7	0.001	N.S.	<0.001***	<0.001***
ILF								
FA, R, mean (SD)	0.420 (0.021)	0.416 (0.016)	0.431 (0.023)	4.82	0.01	N.S.	0.086	0.009**
L, mean (SD)	0.428 (0.021)	0.423 (0.022)	0.432 (0.024)	1.37	0.259	N.S.	N.S.	N.S.
ADC, R, mean (SD)	0.433 (0.021)	0.439 (0.025)	0.422 (0.019)	4.92	0.009	N.S.	N.S.	0.007**
L, mean (SD)	0.440 (0.025)	0.445 (0.028)	0.433 (0.025)	1.689	0.191	N.S.	N.S.	N.S.
IOFF								
FA, R, mean (SD)	0.448 (0.021)	0.446 (0.021)	0.461 (0.022)	4.29	0.016	N.S.	0.066	0.021*
L, mean (SD)	0.451 (0.022)	0.447 (0.024)	0.463 (0.025)	3.93	0.023	N.S.	N.S.	0.02*
ADC, R, mean (SD)	0.431 (0.022)	0.432 (0.025)	0.417 (0.019)	4.53	0.013	N.S.	0.036*	0.023*
L, mean (SD)	0.432 (0.023)	0.438 (0.031)	0.424 (0.022)	2.45	0.092	N.S.	N.S.	0.088

UNC, uncinate fasciculus; ILF, inferior longitudinal fasciculus; IOFF, inferior occipitofrontal fasciculus; FA, fractional anisotrophy; ADC, apparent diffusion coefficient; R, right; L, left; N.S, no significant difference among the group; AD, Alzheimer's disease; NC, normal controls; ANOVA, analysis of variance.

* $p<0.05$.

** $p<0.01$.

*** $p<0.001$.

significant mean ADC increase of the bilateral UNC (right, $p<0.001$; left, $p<0.01$) and the right IOFF ($p<0.05$) at baseline point in AD patients. Furthermore, AD patients showed the significant mean FA reduction of the right ILF ($p<0.01$) and the bilateral IOFF (right, $p<0.05$; left, $p<0.05$), and significant mean ADC increase of the right ILF ($p<0.01$) and the right IOFF ($p<0.05$) at follow-up point.

2.3. D_A and D_R

The mean D_A and D_R values of the UNC, ILF and IOFF for all groups are shown in Table 3. Among the AD patients, the significant mean D_R increase of the left UNC ($p<0.05$) and the marginally significant mean D_R increase of the right UNC were shown at follow-up point rather than at baseline point. In contrast, no other metrics were significant between baseline and follow-up point. Compared with the normal controls, AD patients showed the significant mean D_R increase of the bilateral UNC (right, $p<0.001$; left, $p<0.001$) and the right IOFF ($p<0.05$) at baseline point. Additionally, AD patients showed the significant mean D_R increase of the right ILF ($p<0.01$) and the left IOFF ($p<0.01$) with disease progression.

3. Discussion

The present study explored the white matter microstructural abnormalities in AD patients with disease progression using tractography-based analysis. To the best of our knowledge, this is the first study where AD patients were followed and assessed for longitudinal changes of their white matter bundles. In this study, we found mean FA reduction of the bilateral UNC in the course of clinical follow-up among AD patients. In addition, compared with normal controls, white matter microstructural changes in ILF and IOFF were observed in AD patients. Furthermore, examining the

Table 3 – The mean axial and radial diffusivity of the UNC, ILF and IOFF, and statistical analysis among all the groups.

Variable	Group			One-way ANOVA		Post-hoc Bonferroni Test, p value		
	AD Baseline	AD Follow	NC	F	p value	AD Baseline vs. AD Follow	AD Baseline vs. NC	AD Follow vs. NC
UNC								
Axial, R, mean (SD)	0.608 (0.022)	0.613 (0.029)	0.597 (0.019)	3.59	0.031	N.S.	N.S.	0.029*
L, mean (SD)	0.609 (0.027)	0.611 (0.034)	0.596 (0.019)	2.6	0.079	N.S.	N.S.	N.S.
Radial, R, mean (SD)	0.341 (0.015)	0.351 (0.022)	0.322 (0.015)	20.9	<0.001***	0.053	<0.001***	<0.001***
L, mean (SD)	0.345 (0.016)	0.355 (0.020)	0.321 (0.015)	32.8	<0.001***	0.048*	<0.001***	<0.001***
ILF								
Axial, R, mean (SD)	0.643 (0.026)	0.648 (0.033)	0.633 (0.021)	2.52	0.086	N.S.	N.S.	N.S.
L, mean (SD)	0.659 (0.035)	0.663 (0.035)	0.651 (0.031)	1.01	0.367	N.S.	N.S.	N.S.
Radial, R, mean (SD)	0.332 (0.021)	0.336 (0.023)	0.320 (0.019)	5.14	0.008	N.S.	0.076	0.007**
L, mean (SD)	0.331 (0.024)	0.341 (0.025)	0.327 (0.026)	2.77	0.068	N.S.	N.S.	N.S.
IOFF								
Axial, R, mean (SD)	0.659 (0.026)	0.658 (0.027)	0.648 (0.021)	1.72	0.184	N.S.	N.S.	N.S.
L, mean (SD)	0.662 (0.029)	0.665 (0.043)	0.657 (0.028)	0.49	0.616	N.S.	N.S.	N.S.
Radial, R, mean (SD)	0.322 (0.021)	0.323 (0.028)	0.305 (0.011)	5.83	0.004	N.S.	0.015*	0.007**
L, mean (SD)	0.320 (0.021)	0.328 (0.026)	0.390 (0.022)	5.34	0.006	N.S.	N.S.	0.005**

UNC, uncinate fasciculus; ILF, inferior longitudinal fasciculus; IOFF, inferior occipitofrontal fasciculus; R, right; L, left; AD, Alzheimer's disease; NC, normal controls; ANOVA, analysis of variance; N.S, no significant difference among the groups.
* $p<0.05$.
** $p<0.01$.
*** $p<0.001$.

diffusivity, we found increase of mean radial diffusivity in the bilateral UNC with AD disease progression.

It is known that the UNC connects the orbitofrontal cortex in the frontal lobe and anterior part of the temporal lobe, and plays an important role in memory and cognition (Highley et al., 2002). There have been previous reports of abnormality of the UNC in AD (Taoka et al., 2006; Yasmin et al., 2008). Yasmin et al. reported that AD patients showed a significant FA reduction in the bilateral UNC compared with healthy controls using tract-specific analysis, and Taoka et.al found a significant FA reduction and ADC increase in AD rather than in normal controls using a tract of interest method (Taoka et al., 2006; Yasmin et al., 2008). These results were consistent with our present study. Furthermore, we followed the AD patients and found FA reduction of the UNC with disease progression. This is consistent with a previous study which reported that the FA value of the UNC was positively correlated with the MMSE score and negatively correlated with the ADAS-Cog score in AD with DTI analysis (Morikawa et al., 2010). In AD pathology, the pathophysiological change occurs in the early AD stage in the MTL, which includes the transentorhinal region, entorhinal cortex, and hippocampus, which subsequently spreads to the temporal, parietal and frontal cortex in the disease course (Braak and Braak, 1995). Thus, it is suggested that progressive disruption of the UNC fiber reflects the pathological change due to deterioration in AD which may underlie AD pathophysiology.

In contrast, we found that there was no significant FA reduction or ADC increase in the ILF and the IOFF between baseline and follow-up period. On the other hand, AD patients were found to have significant FA reduction or ADC increase in the ILF of the IOFF compared with normal controls. In previous studies, the diffusion abnormalities of the ILF or the IOFF in AD have been reported, which were consistent with our recent data (Cho et al., 2008; Fellgiebel et al., 2008; Stricker et al., 2009). The ILF connects the occipital lobe with the anterior part of the temporal lobe, and anteriorly joins the UNC to relay information to the orbitofrontal cortex (Catani et al., 2003). Meanwhile, the IOFF connects the occipital, posterior temporal, and the orbitofrontal areas, and also contains fibers that connect the frontal lobe with the posterior part of the parietal and temporal lobes (Taoka et al., 2006). It has been suggested that the ILF and the IOFF are associated with object recognition, visual spatial processing, visual and verbal memory, and visual emotional process (Chanraud et al., 2010; Kiuchi et al., 2010; Kringelbach, 2005). In the course of AD, patients show symptoms of memory impairment and disorientation in the early phase, and consecutively show cognitive decline such as emotional, visuospatial disturbance and loss of executive function. In this study, we observed gradual FA decrease and ADC increase in the ILF and IOFF from normal controls to baseline and follow-up AD patients, which suggested that the progressive microstructural damages to the ILF and the IOFF might be associated with cognitive decline in AD pathology.

Considering the diffusion analysis, we found significant increase in radial diffusivity in UNC among the follow-up rather than baseline among AD patients. Therefore, it was shown to increase the radial diffusivity in ILF and IOFF in AD patients compared with normal controls. In this study, we identified greater increase of radial diffusivity than that of axial diffusivity with disease progression. The previous DTI studies in AD showed an increase of radial diffusivity (Huang

et al., 2007; Salat et al., 2010). This is consistent with our recent examination. Salat et al. reported an increase of radial diffusivity in the medial temporal, occipital, and precuneus in DTI analysis. Moreover, Stricker et al. reported that an increase of radial diffusion reflects a loss of myelin integrity and neural demyelination (Stricker et al., 2009). Progressive white matter axonal demyelination underlies AD pathology, resulting in critical disturbances in neural condition, and thus severely damaging brain function (Roher et al., 2002). Taking these studies together, we considered that our data might reflect these white matter pathological changes in AD.

There are some limitations to the current study. The first limitation is the measurement protocol for diffusion tensor imaging. We applied a 6-axis diffusion encoding gradient, which is a small number for diffusion encoding (Jones, 2004). Because the AD subjects in this study had several problems in their cognitive functions, we needed to set shorter imaging time by using smaller number of diffusion encoding. Furthermore, there is a study which describes that the number of diffusion encoding does not exert any significant effect of visualization of the optic radiation (Yamamoto et al., 2007). This is also the reason for the number of diffusion encoding gradients. The second limitation is that the DTI images were obtained using a 1.5-Tesla MRI system, relatively weak magnetic fields, and the number of participants was comparatively small. We considered that future studies should include a larger number of participants using higher-field MRI system. The third limitation is that the follow-up period among AD patients was incongruent. In this study, AD patients were followed between one and three years. However, in this study, cognitive function in each AD patient did not get worse with disease progression, from mild to moderate stage, and so we thought that there was no remarkable cognitive fluctuation among follow up of the AD patients due to the incongruent follow up period. The fourth limitation is that AD patients in this study were administered choline esterase inhibitors, which might affect somewhat the diffusion measures. We would investigate it in our future analysis.

Table 4 – Definitions of the seed and target regions of interest for each tractography.

	Seed	Target
UNC	In the white matter of the frontal lobe on a coronal plane at the tip of the frontal horn of the lateral ventricle	In the white matter on a coronal plane at the tip of the inferior horn of the lateral ventricle in the ipsilateral temporal tip
ILF	In the white matter on a coronal plane at the tip of the inferior horn of the lateral ventricle in the temporal tip	In the ipsilateral sagittal stratum on a coronal plane at the level of the trigone of the lateral ventricle
IOFF	In the white matter of the frontal lobe on a coronal plane at the tip of the frontal horn of the lateral ventricle	In the ipsilateral sagittal stratum on a coronal plane at the level of the trigone of the lateral ventricle

UNC, uncinate fasciculus; ILF, inferior longitudinal fasciculus; IOFF, inferior occipitofrontal fasciculus.

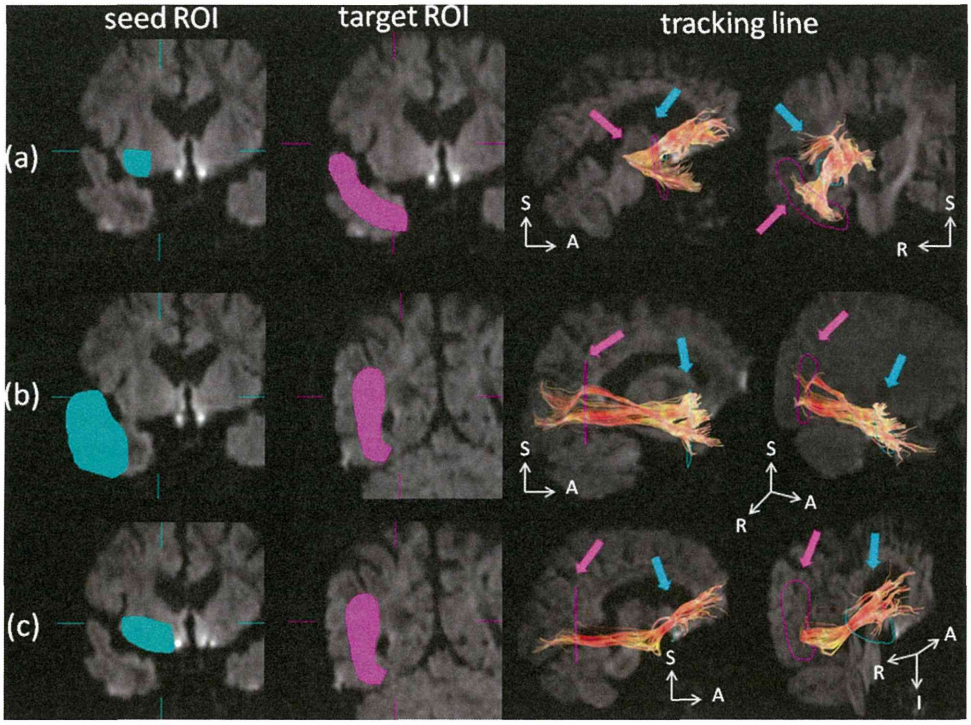

Fig. 1 – Tractography of the (a) uncinate fasciculus (UNC), (b) inferior longitudinal fasciculus (ILF) and (c) inferior occipitofrontal fasciculus (IOFF). The light blue colored object indicates the seed ROI, and the pink one does the target ROI. S; superior, I; inferior, A; anterior, R; right.

In conclusion, we examined the longitudinal evaluation of the microstructural white matter changes in AD patients with DTI tractography analysis. We found diffusion abnormalities in the major white matter bundles with disease progression, which may reflect white matter changes in AD pathology. Therefore, quantifying the histopathological changes to white matter may be a useful biological marker for monitoring AD.

4. Experimental procedures

4.1. Subjects

The subjects in this study were 35 AD patients (11 males and 24 females) with probable AD and age-matched 29 normal controls (12 males and 17 females), recruited from the Department of Psychiatry, Nara Medical University, Kashihara, Japan. Probable AD was diagnosed according to the National Institute of Neurological and Communicative Disorders and Stroke and the Alzheimer's Disease and Related Disorders Association (NINCDS-ADRDA) criteria (McKhann et al., 1984). Among the AD patients, 26 took 5 mg of donepezil, 2 took 10 mg, and 7 patients took no donepezil medication. AD patients who underwent baseline MRI acquisition and cognitive function assessment at the time of initial evaluation were clinically followed up, and underwent secondary evaluation at intervals of about 1.5 years on average. Assessment of cognitive function was examined according to a standardized cognitive battery of tests, including the MMSE and the ADAS-Cog., the reliability and validity of which have previously been confirmed in Japan (Homma et al., 1992). All participants were screened for comorbid medical and psychiatric conditions by means of clinical, physical, and neurological examinations. A somatic and neurological evaluation was undertaken in all subjects, with a routine laboratory examination and brain structural MRI. Exclusion criteria for all of the subjects were a history of substantial head injury, seizures, neurological diseases, impaired thyroid function, and corticosteroid use. Subjects with cortical infarctions on T-2 weighted images were also excluded, whereas subjects with small lacunae in the white matter (fewer than 5 lesions on T2-weighted images) were included. Normal controls were people who had a medical examination and cognitive assessment including the MMSE at Nara Medical University hospital, and we excluded those who met the criteria for probable AD or DSM-IV axis I disorder. All subjects were right handed.

4.2. MRI acquisition

A 1.5-Tesla clinical MRI unit (Magnetom Sonata, Siemens AG, Erlangen, Germany) was used to obtain diffusion tensor images. Diffusion-weighted images were obtained using an echo planner imaging sequence (repetition time (TR)= 4900 ms, echo time (TE)=85 ms, b=1000 s/mm^2, 6-axis encoding, field of view=230 mm, matrix=128 × 128, slice thickness 3 mm with no gap, averaging=6). We obtained 39 to 50 continuous slice images, covering the whole brain. We also acquired regular structural T1-weighted (spine-echo TR=500, TE=20) and T2-weighted (turbo spine-echo TR=4000, TE=110) images.

4.3. Image analysis

Tractographies were created using Volume One and dTV II DTI softwares developed by Masutani et al. (2003) University of Tokyo, Diffusion Tensor Visualizer ver. 2; available at (http://www.ut-radiology.umin.jp/people/masutani/dTV.htm). Interpolation along the z-axis was performed to obtain isotropic data (voxel size, 0.89 × 0.89 × 0.89 mm). The eigen vector associated with the largest eigenvalue or the principal axis was assumed to represent the local fiber direction. The tracking algorithm moved along the principal axis. The diffusion tensor at the next location was determined from the adjacent voxels, and its principal axis was subsequently estimated. Tracking lines were traced in this way, and propagated in both anterograde and retrograde directions until the FA fell below an assigned threshold. The settings for each tractography were as follows: the FA threshold for tracking was set at 0.18, the stop length was set at 160 steps and the seed and target ROIs are given in Table 4. Using these data, we delineated the bilateral UNC, ILF and IOFF (Fig. 1). The dTV II software has a function that calculates the mean FA, mean ADC (10^{-3} s/mm^2), mean D_A (10^{-3} s/mm^2) and mean D_R (10^{-3} s/mm^2) along the constructed tract. We measured them along each tractography.

4.4. Statistical analysis

Data were analyzed using the Statistical Package for Social Science (SPSS for Windows 16.0; SPSS, Chicago, Illinois). Statistical analyses were performed on FA, ADC, D_A and D_R values by one-way analysis of variance (ANOVA) with follow up post-hoc Bonferroni test.

Acknowledgment

We thank Mr. Jose M. Morales who kindly assist with reading of the abstract. We also thank all colleagues and participants in the recent study.

REFERENCES

Basser, P.J., Pierpaoli, C., et al., 1998. A simplified method to measure the diffusion tensor from seven MR images. Magn. Reson. Med. 39, 928–934.

Bozzali, M., Padovani, A., Caltagirone, C., Borroni, B., et al., 2011. Regional grey matter loss and brain disconnection across Alzheimer disease evolution. Curr. Med. Chem. 18, 2452–2458.

Braak, H., Braak, E., et al., 1995. Staging of Alzheimer's disease-related neurofibrillary changes. Neurobiol. Aging 16, 271–278.

Catani, M., Jones, DK., Donato, R., Ffytche, D.H., et al., 2003. Occipito–temporal connections in the human brain. Brain 126, 2093–2107.

Chanraud, S., Zahr, N., Sullivan, E.V., Pfefferbaum, A., et al., 2010. MR diffusion tensor imaging: a window into white matte integrity of the working brain. Neuropsychol. Rev. 20, 209–225.

Chen, T.F., Lin, C.C., Chen, Y.F., Liu, H.M., Hua, M.S., Huang, Y.C., Chiu, M.J., et al., 2009. Diffusion tensor changes in patients with amnesic mild cognitive impairment and various dementias. Psychiatry Res. 173, 15–21.

Cho, H., Yang, D.W., Shon, Y.M., Kim, B.S., Kim, Y.I., Choi, Y.B., Lee, K.S., Shim, Y.S., Yoon, B., Kim, W., Ahn, K.J., et al., 2008. Abnormal integrity of corticocortical tracts in mild cognitive impairment: a diffusion tensor imaging study. J. Korean Med. Sci. 23, 477–483.

Delbeuck, X., Collette, F., Van. Der. Linden, M., et al., 2007. Is Alzheimer's disease a disconnection syndrome? Evidence from a crossmodal audio–visual illusory experiment. Neuropsychologia 45, 3315–3323.

Di. Paola, M., Macaluso, E., Carlesimo, G.A., Tomaiuolo, F., Worsley, K.J., Fadda, L., Caltagirone, C., et al., 2007. Episodic memory impairment in patients with Alzheimer's disease is correlated with entorhinal cortex atrophy. A voxel-based morphometry study. J. Neurol. 254, 774–781.

Fellgiebel, A., Schermuly, I., Gerhard, A., Keller, I., Albrecht, J., Weibrich, C., Müller, M.J., Stoeter, P., et al., 2008. Functional relevant loss of long association fibre tracts integrity in early Alzheimer's disease. Neuropsychologia 46, 1698–1706.

Highley, J.R., Walker, M.A., Esiri, M.M., Crow, T.J., Harrison, P.J., et al., 2002. Asymmetry of the uncinate fasciculus: a post-mortem study of normal subjects and patients with schizophrenia. Cereb. Cortex 12, 1218–1224.

Hong, Y.J., Yoon, B., Shim, Y.S., Cho, A.H., Lim, S.C., Ahn, K.J., Yang, D.W., et al., 2010. Differences in microstructural alterations of the hippocampus in Alzheimer disease and idiopathic normal pressure hydrocephalus: a diffusion tensor imaging study. Am. J. Neuroradiol. 31, 1867–1872.

Homma, A., Fukuzawa, K., Tsukada, Y., Ishii, T., Hasegawa, K., Mohs, R.C., et al., 1992. Development of a Japanese version of Alzheimer's disease Assessment Scale (ADAS). Jpn. J. Geriatr. Psychiatry 3, 647–655.

Huang, J., Friedland, R.P., Auchus, A.P., et al., 2007. Diffusion tensor imaging of normal-appearing white matter in mild cognitive impairment an early Alzheimer disease: preliminary evidence of axonal degeneration in the temporal lobe. Am. J. Neuroradiol. 28, 1943–1948.

Jones, D.K., et al., 2004. The effect of gradient sampling schemes on measures derived from diffusion tensor MRI: a Monte Carlo study. Magn. Reson. Med. 51, 807–815.

Kiuchi, K., Morikawa, M., Taoka, T., Nagashima, T., Yamauchi, T., Makinodan, M., Norimoto, K., Hashimoto, K., Kosaka, J., Inoue, Y., Inoue, M., Kichikawa, K., Kishimoto, T., et al., 2009. Abnormalities of the uncinate fasciculus and posterior cingulate fasciculus in mild cognitive impairment and early Alzheimer's disease: a diffusion tensor tractography study. Brain Res. 1287, 184–191.

Kiuchi, K., Morikawa, M., Taoka, T., Kitamura, S., Nagashima, T., Makinodan, M., Nakagawa, K., Fukusumi, M., Ikeshita, K., Inoue, M., Kichikawa, K., Kishimoto, T., et al., 2010. White matter changes in dementia with Lewy bodies and Alzheimer's disease: a tractography based study. J. Psychiatry Res. 45, 1095–1100.

Kobayashi, K., Hayashi, M., Nakano, H., Fukutani, Y., Sasaki, K., Shimazaki, M., Koshino, Y., et al., 2002. Apoptosis of astrocytes with enhanced lysosomal activity and oligodendrocytes in white matter lesions in Alzheimer's disease. Neuropathol. Appl. Neurobiol. 28, 238–251.

Kringelbach, M.L., et al., 2005. The human orbitofrontal cortex: linking reward to hedonic experience. Nat. Rev. Neurosci. 6, 691–702.

Masutani, Y., Aoki, S., Abe, O., Hayashi, N., Otomo, K., et al., 2003. MR diffusion tensor imaging: recent advance and new techniques for diffusion tensor visualization. Eur. J. Radiol. 46, 53–66.

Matsuda, H., Kitayama, N., Ohnishi, T., Asada, T., Nakano, S., Sakamoto, S., Imabayashi, E., Katoh, A., et al., 2002. Longitudinal evaluation of both morphologic and functional changes in the same individuals with Alzheimer's disease. J. Nucl. Med. 43, 304–311.

McKhann, G., Drachman, D., Folstein, M., Katzman, R., Price, D., Stadlan, E.M., et al., 1984. Clinical diagnosis of Alzheimer's disease: report of the NINCDS-ADRDA Work Group under the auspices of Department of Health and Human Services Task Force on Alzheimer's Disease. Neurology 34, 939–944.

Morikawa, M., Kiuchi, K., Taoka, T., Nagauchi, K., Kichikawa, K., Kishimoto, T., et al., 2010. Uncinate fasciculus-correlated cognition in Alzheimer's disease: a diffusion tensor imaging study by tractography. Psychogeriatrics 10, 15–20.

Nakata, Y., Sato, N., Abe, O., Shikakura, S., Arima, K., Furuta, N., Uno, M., Hirai, S., Masutani, Y., Ohtomo, K., Aoki, S., et al., 2008. Diffusion abnormality in posterior cingulate fiber tracts in Alzheimer's disease: tract-specific analysis. Radiat. Med. 26, 466–473.

Pievani, M., Agosta, F., Pagani, E., Canu, E., Sala, S., Absinta, M., Geroldi, C., Ganzola, R., Frisoni, G.B., Filippi, M., et al., 2010. Assessment of white matter tract damage in mild cognitive impairment and Alzheimer's disease. Hum. Brain Mapp. 31, 1862–1875.

Roher, A.E., Weiss, N., Kokjohn, T.A., Kuo, Y.M., Kalback, W., Anthony, J., Watson, D., Luehrs, D.C., Sue, L., Walker, D., Emmerling, M., Goux, W., Beach, T., et al., 2002. Increased A beta peptides and reduced cholesterol and myelin proteins characterize white matter degeneration in Alzheimer's disease. Biochemistry 41, 11080–11090.

Rose, S.E., Janke, A.L., Chalk, J.B., et al., 2008. Gray and white matter changes in Alzheimer's disease: a diffusion tensor imaging study. J. Magn. Reson. Imaging 27, 20–26.

Roth, A.D., Ramírez, G., Alarcón, R., Von. Bernhardi, R., et al., 2005. Oligodendrocytes damage in Alzheimer's disease: beta amyloid toxicity and inflammation. Biol. Res. 38, 381–387.

Salat, D.H., Tuch, D.S., van. der. Kouwe, A.J., Greve, D.N., Pappu, V., Lee, S.Y., Hevelone, N.D., Zaleta, A.K., Growdon, J.H., Corkin, S., Fischl, B., Rosas, H.D., et al., 2010. White matter pathology isolates the hippocampal formation in Alzheimer's disease. Neurobiol. Aging 31, 244–256.

Song, S.K., Sun, S.W., Ramsbottom, M.J., Chang, C., Russell, J., Cross, A.H., et al., 2002. Dysmyelination revealed through MRI as increased radial (but unchanged axial) diffusion of water. Neuroimage 17, 1429–1436.

Stricker, N.H., Schweinsburg, B.C., Delano-Wood, L., Wierenga, C. E., Bangen, K.J., Haaland, K.Y., Frank, L.R., Salmon, D.P., Bondi, M.W., et al., 2009. Decreased white matter integrity in late-myelinating fiber pathways in Alzheimer's disease supports retrogenesis. Neuroimage 45, 10–16.

Sun, S.W., Song, S.K., Harms, M.P., Lin, S.J., Holtzman, D.M., Merchant, K.M., Kotyk, J.J., et al., 2005. Detection of age-dependent brain injury in a mouse model of brain amyloidosis associated with Alzheimer's disease using magnetic resonance diffusion tensor imaging. Exp. Neurol. 191, 77–85.

Taoka, T., Iwasaki, S., Sakamoto, M., Nakagawa, H., Fukusumi, A., Myochin, K., Hirohashi, S., Hoshida, T., Kichikawa, K., et al., 2006. Diffusion anisotrophy and diffusivity of white matter tracts within the temporal stem in Alzheimer disease: evaluation of the "tract of interest" by diffusion tensor tractography. Am. J. Neuroradiol. 27, 1040–1045.

Yamamoto, A., Miki, Y., Urayama, S., Fushimi, Y., Okada, T., Hanakawa, T., Fukuyama, H., Togashi, K., et al., 2007. Diffusion tensor fiber tractography of the optic radiation: analysis with 6-, 12-, 40-, and 81-directional motion-probing gradients, a preliminary study. Am. J. Neuroradiol. 28, 92–96.

Yasmin, H., Nakata, Y., Aoki, S., Abe, O., Sato, N., Nemoto, K., Arima, K., Furuta, N., Uno, M., Hirai, S., Masutani, Y., Ohtomo, K., et al., 2008. Diffusion abnormalities of the uncinate fasciculus in Alzheimer's disease: diffusion tensor tract-specific analysis using a new method to measure the core of the tract. Neuroradiology 50, 293–299.